International Journal of Nanomedicine Dovepress

Open Access Full Text Article ORIGINAL RESEARCH

Polyoxometalates Ameliorate Metabolic Dysfunction-Associated Steatotic Liver Disease by Activating the AMPK Signaling Pathway

Dandan Wang[1–3,*], Jingguo Wang[3,*], Zequn Yin[4], Ke Gong[3], Shuang Zhang[3], Zhengbao Zha[3], Yajun Duan[4]

[1]School of Pharmacy, Anhui University of Chinese Medicine, Hefei, Anhui, 230011, People's Republic of China; [2]State Key Laboratory of Functions and Applications of Medicinal Plants, Guizhou Medical University, Guiyang, 550014, People's Republic of China; [3]School of Food and Biological Engineering, Hefei University of Technology, Hefei, Anhui, 230601, People's Republic of China; [4]Department of Cardiology, The First Affiliated Hospital of USTC, Division of Life Sciences and Medicine, University of Science and Technology of China, Hefei, Anhui, 230031, People's Republic of China

*These authors contributed equally to this work

Correspondence: Zhengbao Zha, School of Food and Biological Engineering, Hefei University of Technology, No. 420 Feicui Road, Hefei, Anhui, 230601, People's Republic of China, Email zbzha@hfut.edu.cn; Yajun Duan, Department of Cardiology, The First Affiliated Hospital of USTC, Division of Life Sciences and Medicine, University of Science and Technology of China, No. 96 Jinzhai Road, Hefei, Anhui, 230031, People's Republic of China, Email yajunduan@ustc.edu.cn

Introduction: Metabolic dysfunction-associated steatotic liver disease (MASLD), the most prevalent chronic liver disorder, has garnered increasing attention globally owing to its associated health complications. However, the lack of available therapeutic medications and inadequate management of complications in metabolic dysfunction-associated steatohepatitis (MASH) present significant challenges. There are little studies evaluating the effectiveness of POM in treating MASLD. In this study, we synthesized polyoxometalates (POM) for potential treatment of MASLD.

Methods: We induced liver disease in mice using two approaches: feeding a high-fat diet (HFD) to establish MASLD or feeding a methionine–choline deficient (MCD) diet to induce hepatic lipotoxicity and MASH. Various metabolic parameters were detected, and biochemical and histological evaluations were conducted on MASLD. Western blotting, qRT-PCR and immunofluorescence assays were used to elucidate the molecular mechanism of POM in the treatment of MASLD.

Results: POM therapy resulted in significant improvements in weight gain, dyslipidemia, liver injury, and hepatic steatosis in mice fed a HFD. Notably, in a more severe dietary-induced MASH model with MCD diet, POM significantly attenuated hepatic lipid accumulation, inflammation, and fibrosis. POM treatment effectively attenuated palmitic acid and oleic acid-induced lipid accumulation in HepG2 and Huh7 cells by targeting the AMPK pathway to regulate lipid metabolism, which was confirmed by AMPK inhibitor. Additionally, the activation of AMPK signaling by POM suppressed the expression of lipid synthesis genes, including sterol regulatory element-binding protein 1c (SREBP1c) and SREBP2, while concurrently upregulating the expression of sirtuin 1 (SIRT1) to promote fatty acid oxidation.

Conclusion: These findings suggest that POM is a promising therapeutic strategy with high efficacy in multiple MASLD models.

Keywords: polyoxometalates, MASLD, MASH, AMPK, lipotoxicity

Introduction

Metabolic dysfunction-associated steatotic liver disease (MASLD) is a growing global health issue characterized by the accumulation of fat in at least 5% of the hepatocytes. It is closely linked to metabolic syndrome, with strong associations to both obesity and diabetes. By 2030, over 30% of adults are expected to develop MASLD.[1] MASLD is a chronic liver disease ranging from simple steatosis to more severe metabolic dysfunction-associated steatohepatitis (MASH), which is accompanied by progressive hepatocellular ballooning, inflammation, fibrosis and eventually hepatocellular carcinoma

Received: 1 July 2024
Accepted: 17 October 2024
Published: 25 October 2024

Graphical Abstract

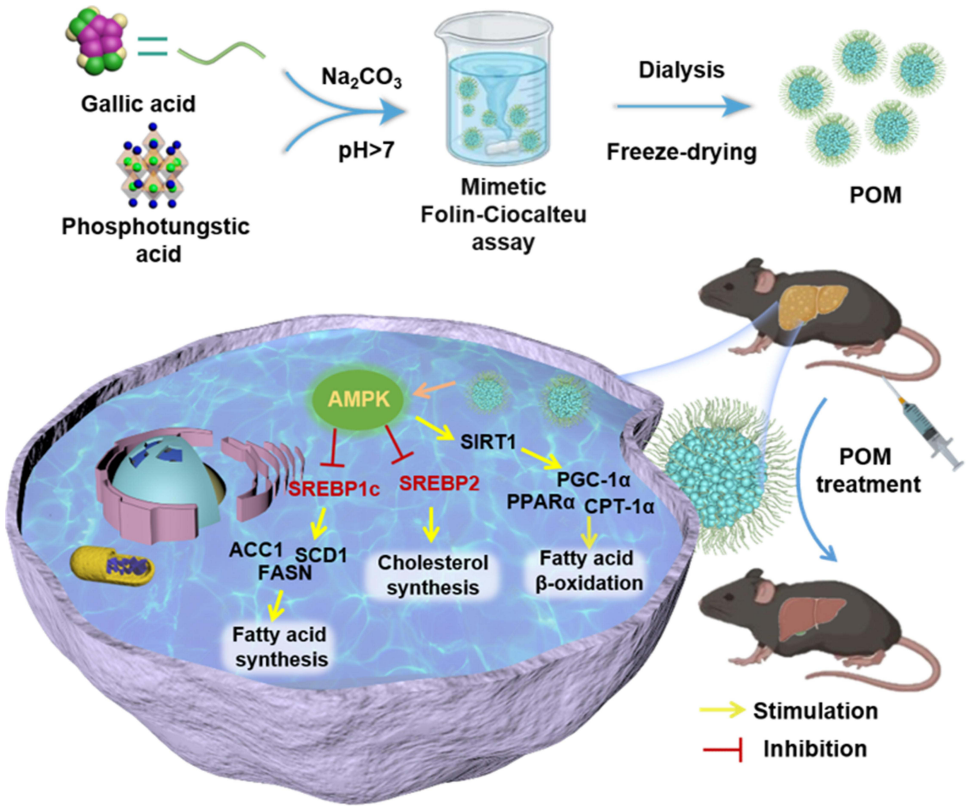

(HCC).[2,3] While intensive dietary adjustments, lifestyle modifications, or bariatric surgery may be effective treatments, these approaches are often inadequate for individuals with advanced stages of the disease. Among the most promising drugs in development for treating MASH are PPAR agonists. However, despite their potential, no currently available PPAR agonist has shown satisfactory success in resolving NASH.[4] Therefore, there is an urgent need to identify effective medicines and bioactive compounds for the treatment of MASLD.

Increasingly, studies have indicated that liver lipid accumulation is a key initial stage of MASLD.[5] The accumulation of fatty acids in hepatocytes promotes the production of lipotoxic substances, leading to oxidative stress and inflammatory responses.[6] The inflammatory response activates stellate cells to promote hepatic fibrosis and exacerbate lipotoxic conditions in hepatocytes.[7] The liver plays a pivotal role in regulating energy homeostasis and is extremely vulnerable to the effects of high-fat diet (HFD) or methionine–choline deficient (MCD) diet. Excessive lipid accumulation in hepatocytes may be caused by four main metabolic disorders: (1) increased uptake of fatty acids by hepatocytes, (2) increased *de novo* lipogenesis, (3) reduced fatty acid oxidation or lipid droplet autophagy, and (4) impaired export from hepatocytes to blood of triglycerides (TG).[8] Consequently, therapies capable of intervening in these processes may be effective in the treatment of MASLD.

AMP-activated protein kinase (AMPK) responds to various anabolic pathways and stimulates catabolic pathways to balance ATP production with cellular demand. In the liver, AMPK activation downregulates the activity of acetyl-CoA carboxylase 1 (ACC1) and sterol regulatory element-binding protein 1c (SREBP1c), thereby inhibiting fatty acid and TG synthesis.[9] In addition, AMPK altered Sirtuin 1 (SIRT1) activity by regulating the intracellular level of its co-substrate NAD+.[10] SIRT1 is a (NAD+)-dependent deacetylase that serves as an important metabolic regulator.[11] Research has shown that increasing expression of SIRT1 can alleviate obesity in HFD-induced mice by reducing acetylation of peroxisome proliferator-activated receptor (PPAR) γ coactivator 1α (PGC-1α) and forkhead box O3 (FoxO3).[12,13]

SIRT1 regulates lipid homeostasis by positively regulating PPARα signaling primarily through the activation of PGC-1α, as a transcriptional co-activator interacts with PPARα to enhances PPARα -mediated transcriptional activation.[14] Most identified PPARα target genes are involved in liver fatty acid β-oxidation, including acyl-CoAoxidase1 (ACOX1) and carnitine palmitoyl transferase −1α (CPT-1α).[15] AMPK regulates the expression of lipid metabolism genes through the modulation of PGC-1α activity by SIRT1.[13] In addition, AMPK promotes hepatic lipid metabolism, up-regulates mitochondrial respiration and increased flux of PPARα and CPT-1α from β-oxidation.[16] Thus, AMPK plays a vital role in regulating lipid metabolism in MASLD.

The development of nanomanufacturing technology has yielded a variety of nanodrugs such as nanoemulsions, inorganic nanoparticles, and liposomes, which have been used in the diagnosis and treatment of acute hepatitis, drug-induced liver injury, and MASLD.[17,18] The application of cerium oxide nanoparticles to CCl_4-induced rats decreased portal hypertension and steatosis, and lowered inflammatory responses.[18] Cao et al prepared fenofibrate nanoliposomes, which were shown to prevent and treat MASLD by increasing fenofibrate plasma concentrations and significantly reducing excess hepatic lipids.[19] These exciting results make nanomedicines an exciting opportunity to develop novel therapies for MASLD. However, slow degradation, potential systemic side effects, and expensive and time-consuming production processes have severely limited some nanomedicines from reaching their expected potential.[20–22]

Polyoxometalates (POM) were initially synthesized for tumor treatment; however, their limited bioavailability and toxic side effects have hindered their further application.[23] With advancements in synthesis methodology, researchers have developed various reducing and protective agents to address these challenges.[24] Huang et al utilized the ascorbic acid reduction method to synthesize phosphomolybdic acid-POM, which was subsequently applied in the context of acute kidney injury.[25] The POM synthesized by Zha et al, using gallic acid as a protective agent, not only exhibits potent tumor inhibitory effects but also demonstrates negligible acute or chronic toxicity towards mice.[26] The addition of gallic acid further enhances the in vivo circulation time of POM, thereby improving its bioavailability. This attribute is particularly advantageous for enhancing therapeutic efficacy. Furthermore, the potential applications of POM extend beyond tumor therapy and include Alzheimer's disease and colitis.[27] However, no studies have evaluated the effectiveness of POM in treating MASLD.

In this study, we assessed the potential therapeutic efficacy and molecular mechanisms of POM in HFD-induced MASLD with simple steatosis and MCD-induced hepatic steatohepatitis and fibrosis (MASH). POM treatment inhibited HFD-induced body weight gain, dyslipidemia, liver injury, and hepatic steatosis, whereas in the more severe MCD-induced MASH model, POM significantly decreased lipid accumulation, inflammation, and fibrosis. We showed that POM alleviates MASLD by activating AMPK signaling, which inhibits the expression of lipid synthesis genes and upregulates fatty acid oxidation. Our findings indicated that POM is a promising therapeutic approach for the treatment of MASLD.

Materials and Methods

Materials

Huh7 and HepG2 cells were obtained from ATCC (Manassas, VA, USA). Rabbit anti-ACC1 (Cat# 4190S) polyclonal antibody was supplied by Cell Signaling Technology (Danvers, MA, USA). Rabbit anti-Lamin A/C (Cat# A0249), AMPKα (Cat# A12718), SOD1 (Cat# A0274), SREBP2 (Cat# A4123), FASN (Cat# A0461), SOD2 (Cat# A1340), IL-1β (Cat# A17361), PPARα (Cat# A6697), β-actin (Cat# AC026) antibodies, mouse anti-GAPDH (Cat# AC033) antibody and phospho-AMPKα (Cat# AP0432) antibody were supplied by Abclonal (Boston, USA). Rabbit anti-HSP90 (Cat# 13171-1-AP), FoxO3a (Cat# 10849-1-AP), Bax (Cat# 50599-2-Ig), Bcl-2 (Cat# 12789-1-AP), SCD1 (Cat# 23393-1-AP), SREBP1c (Cat# 14088-1-AP), LXRα (Cat# 14351-1-AP), LXRβ (Cat# 14278-1-AP), Col1a1 (Cat# 14695-1-AP), α-SMA (Cat# 55135-1-AP), Caspase 3 (Cat# 19677-1-AP) antibodies, mouse anti-TNFα (Cat# 60291-1-lg) antibody and FITC-conjugated goat anti-rabbit IgG (H+L) antibody (Cat# SA00003-2) were acquired from Proteintech (Chicago, USA). Rabbit anti-SREBP1c antibody (Cat# ER1917-19) was procured from HuaAn Biotechnology (Zhejiang, China). Rabbit anti-SIRT1 (Cat# DF6033), HMGCR (Cat# DF6518), CPT-1α (Cat# DF12004), PGC-1α (Cat# AF5395) antibodies and phospho-NF-κB p65 (Cat# AF2006) phosphorylated antibody

were obtained from Affinity Biosciences (Cincinnati, OH, USA). Compound C (Cat # HY-13418A) was obtained from MedChem Express (NJ, USA). Mouse TNFα ELISA kit was procured from Sino Biological (Beijing, China). Mouse IL-6 ELISA kit was procured from Ruixin Biotech (Fujian, China). LabAssay Triglyceride were procured from Wako Pure Chemical Industries, Ltd. (Osaka, Japan). Total cholesterol assay kit was procured from Applygen Technologies (Beijing, China). Free fatty acid assay kit was procured from Solarbio Life Sciences (Beijing, China). Dihydroethidium (DHE) was purchased from Yeasen (Shanghai, China). All other reagents were supplied by Sigma-Aldrich (St Louis, MO), except indicated.

Synthesis of POM

POM was synthesized according to reported methods.[26] Briefly, $H_3O_{40}PW_{12}{\cdot}xH_2O$ (60 mg/mL, 1 mL) was added to a solution containing 100 mg gallic acid and stirred for 5 min. Then, sodium carbonate solution (7.5%, 3 mL) was added to the mixture and allowed to react for 5 h. A Purified POM powder was obtained by successive dialysis and freeze-drying.

Cell Culture and Treatment

HepG2 and Huh7 cells were grown in Dulbecco's Modified Eagle's medium (DMEM) supplemented with 10% fetal bovine serum (FBS) and 50 μg/mL penicillin and streptomycin in a humidified atmosphere at 37 °C with 5% CO_2. The cytotoxicity of POM was determined using the MTT method.[28] To induce steatosis in cultured hepatocytes, the cells were treated with palmitic acid (PA, 0.5 mM) and oleic acid (OA, 1.0 mM) for 24 h, with an equal amount of ethanol/BSA (5%) administered to the control cluster.[29] At the same time, cells were treated with different concentration of POM (0, 2.5, 5, 10 μg/mL) for 24 h. After treatment, the cells were fixed with 4% paraformaldehyde for 30 min and stained with an Oil Red O solution. The cells were visualized and photographed using an electron microscope. Cell lysates were examined to characterize TG levels using a kit following the manufacturer's instructions.

qRT–PCR Analysis

Total RNA was isolated from cells and mouse livers using the Total RNApure Reagent (Zomanbio, Beijing, China). After treatment, HepG2 cells (1×10^6 cells/well) or 30 mg mouse liver were lysed by adding 200 μL and 500 μL Total RNApure Reagent, respectively. Mix the lysate thoroughly with chloroform and centrifuge for 10 min (12,000× g, 4°C). The top aqueous phase was collected and mixed with isopropanol to precipitate the total RNA. Complementary DNAs was synthesized with 1 μg RNA using a reverse transcription kit (Vazyme, Nanjing, China). qRT–PCR was performed using SYBR Green PCR Master Mix. Comparative gene expression levels were normalized to those of GAPDH. Fold changes in gene expression were computed with the $2^{-\Delta\Delta ct}$ approach. The qRT–PCR primer sequences are listed in Supplemental Table 1.

Western Blot and Immunofluorescence

Protein expression of FASN, ACC1, SCD1, SREBP1c, LXRα, LXRβ, SIRT1, PGC-1α, PPARα, CPT-1α, total AMPKα, phosphorylated AMPKα, SREBP2, Col1a1, α-SMA, TNFα, IL-1β, phosphorylated NF-κB, FoxO3a, SOD1, SOD2, Bcl-2, Bax, and caspase-3 in the total cell lysate was determined by Western blot as described.[30] In brief, HepG2 cells (1×10^6 cells/well) or 30 mg mouse liver were lysed by adding 200 μL and 500 μL RIPA lysis buffer, respectively. The lysate was centrifuged for 10 min (12,000× g, 4°C). Collecting the supernatant is the protein solution. An equal amount of protein (20~50 μg) from each sample was separated by SDS-PAGE gels and transferred to NC membrane. The membrane was blocked with 5% nonfat dry milk for 2 h and incubated with primary antibody for 12 h at 4°C. Then the membranes were washed three times for 8 min with PBST (PBS containing 0.5% Tween 20). The membranes were incubated with horseradish peroxidase (HRP)-conjugated secondary antibodies for 2 h at room temperature. The band was visualized by efficient chemiluminescence kit (ECL) and the band intensities were quantified using ImageJ software. The quantitative statistical data of Western blot assays are listed in Supplemental Tables 2–8 To assess the nuclear LXRα levels, cells were collected and lysed using a Nuclear and Cytoplasmic Protein Extraction Kit (Keygen Biotech, China). The amount of cellular LXRα was determined by immunofluorescence staining previously outlined.[31]

In vivo Studies

Animal experiments were approved by the Animal Ethics Committee of the Anhui University of Chinese Medicine (No. AHUCM-mouse-2023147) and performed according to the "Guide for the Care and Use of Laboratory Animals" from the National Institutes of Health (NIH). Eight-week-old male C57BL/6J mice were obtained from GemPharmatech Co. Ltd. (China). The mice were separated into 8 groups randomly (5 mice per group). For the HFD model, the mice were fed a 45% fat diet (HFD; Research Diets, D12451) for 10 weeks. To establish the fibrosis model, mice were fed an MCD diet (Research Diets, D12052) for 4 weeks. The mice in the normal group were fed normal chow. The mice were treated with 50 mg/kg body weight POM or an equal amount of saline via tail vein injection once a week. Body weight was assessed at different time points throughout the experiment. At the end of the experiment, the mice were anesthetized and euthanized in a CO_2 chamber, with subsequent collection of blood from eye socket or tissue samples. The serum samples were separated from blood samples by centrifuged for 20 min and stored at −20°C. Low-density lipoprotein cholesterol (LDL-C), total cholesterol (TC), TG, alanine aminotransferase (ALT), aspartate aminotransferase (AST), and alkaline phosphatase (ALP) levels in the serum were measured using an automatic bioanalyzer Model 3100 (Hitachi High-Technologies Corporation, Japan). Free fatty acid (FFA) levels in the mouse serum and liver were measured using a kit.

Measurement of Hepatic Steatosis

To determine TC, FFA, and TG levels in the liver, liver segments were homogenized and lipid levels were assessed using commercial assay kits following the manufacturer's instructions. Cryosections of mouse livers (5 μm) were incubated with Oil Red O (37 °C, 30 min). Liver tissues were dehydrated, embedded in paraffin, and sliced into 5-μm thick sections for staining with hematoxylin and eosin (H&E) to examine morphology, Sirius Red to assess fibrosis, and DHE to examine levels of reactive oxygen species (ROS). Three parallel sections were set for each mouse slice and imaging was evaluated in three distinct fields.

RNA-Seq Analysis

Total RNA was isolated from cells and flash-frozen livers using total RNApure reagent according to the manufacturer's instructions. Transcriptome sequencing experiments were performed by Majorbio Bio-Pharm Biotechnology Co. Ltd. (Shanghai, China). RNA–seq data were assessed using the Majorbio Cloud Platform and Deseq2 R package for differential gene expression analysis. Genes with a fold change in expression of ≥ 2 and $P < 0.05$, between treatment groups, were selected as differentially expressed genes (DEGs). Kyoto Encyclopedia of Genes and Genomes (KEGG) analysis was conducted to assess the pathways and functions of DEGs.

Immunohistochemical Staining

To characterize the expression levels of the target proteins by immunohistochemistry (IHC), paraffin sections of the liver were initially deparaffinized, hydrated, and mixed with antibodies (primary and secondary). After incubation, the sections were subjected to hematoxylin solution and mounted. Three parallel sections were set for each mouse slice and imaging was evaluated in three distinct fields. The images were captured using an electron microscope.

Statistical Analysis

Experiments were conducted with a minimum of three biological replicates. Data are presented as mean ± SEM. All statistical analyses were conducted using the Prism software. Statistical significance was determined using a two-tailed unpaired Student's *t*-test for comparisons between two groups and a one-way ANOVA of variance with a post hoc test for comparisons between two groups. Statistical significance was set at a threshold of $P < 0.05$.

Results

Synthetic Characterization and in vivo Distribution of POM

Transmission electron microscopy (TEM) images of the POM synthesized using our previously reported method showed uniform monodisperse nanostructures (Supplemental experimental sections).[26] Analysis with ImageJ determined that the

average particle size of POM was about 2.27 ± 0.14 nm (Figure 1a); however, owing to the presence of surface gallic acid, the particle size of the POM was determined to be 8.58 ± 0.43 nm with a potential of approximately −27.5 mv (Supplemental Figure S1a). The stretching vibration of the carboxyl group, P–Oa stretching vibration, and the presence of C, O, P, and W in POM were verified using Fourier-transform infrared spectroscopy (FT-IR) and X-ray photoelectron spectroscopy (XPS), respectively (Figure 1b and c). As shown in Supplemental Figure S1b, the absorbance of POM was positively correlated with its concentration, with a peak at approximately 613 nm. Stability is crucial for the preservation and application of POM. Therefore, hydrodynamic and UV absorption were measured to evaluate the stability of POM in different solution environments. Notably, POM displayed excellent stability for up to 7 days (Supplemental Figure S2a and b).

We first evaluated the biodistribution of POM in mice. After tail vein administration of POM, major organs and blood were collected at specific time points and weighed for tissue nitrification (Supplemental experimental sections). The blood activity–time course curve of POM after a single 50 mg/kg tail vein injection showed a bi-exponential distribution (Figure 1d). Two-compartment model fitting results showed that the mean plasma distribution half-life ($t_{1/2}\alpha$) and terminal elimination half-life ($t_{1/2}\beta$) were measured to be 0.24 h and 2.92 h, respectively, suggesting prompt blood clearance of the introduced POM. POM was found to penetrate the liver as early as 2 h post-injection, with the highest accumulation of 22.62 ± 0.94% of the injected dose per gram of tissue (%ID/g), which was essential for the potential amelioration of MASLD (Figure 1e). Additionally, POM was significantly enriched in the kidneys at 2 and 4 h, indicating that POM with smaller hydrodynamic diameters could be cleared by the kidneys (Figure 1e).

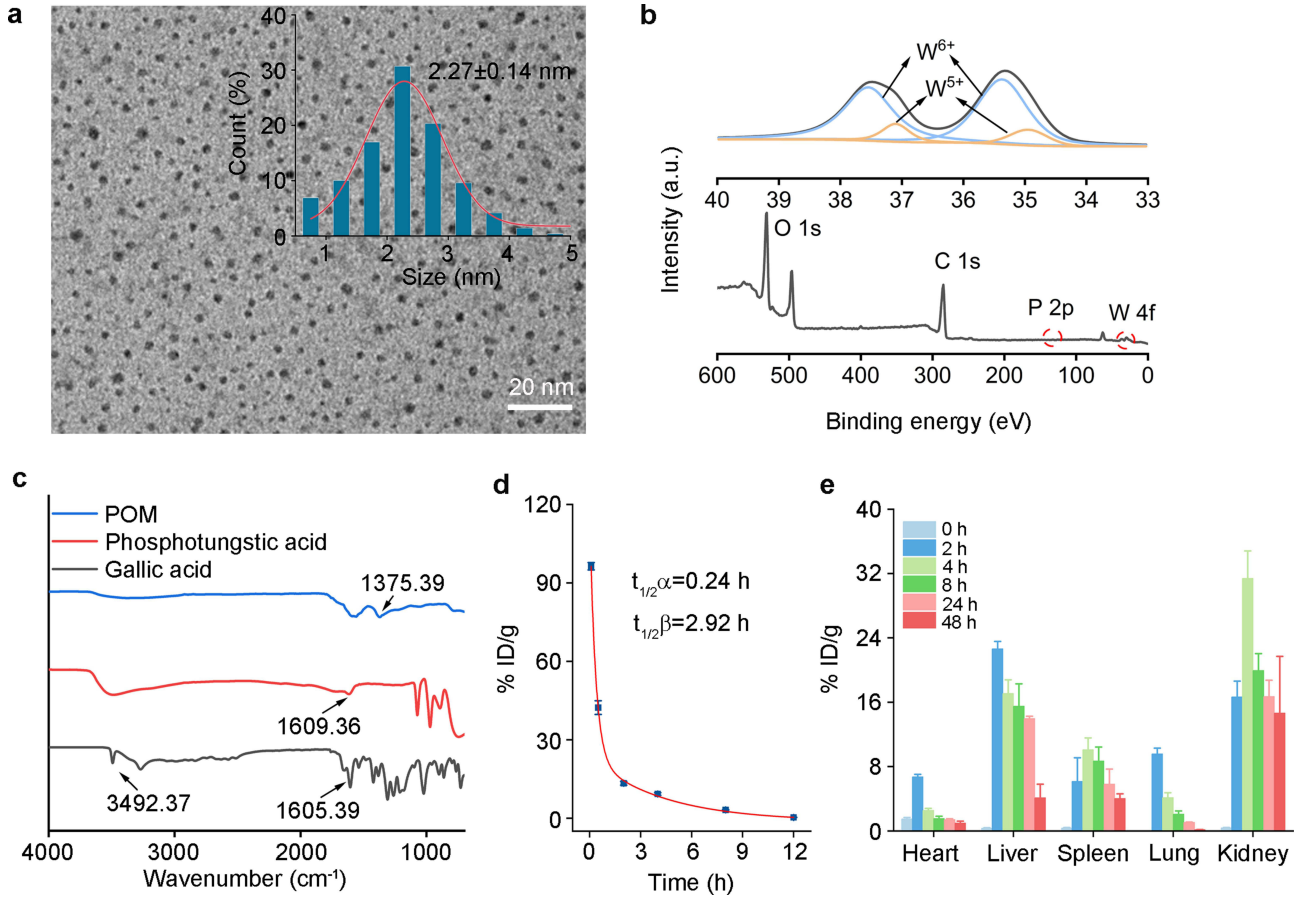

Figure 1 Characterization and biodistribution of POM. (**a, b**) TEM image (magnification: 150000x; inset: diameter distribution curve) and XPS spectra of POM. (**c**) FT-IR spectra. (**d**) Blood circulation and (**e**) biodistribution of POM in major organs in vivo.

POM Ameliorate HFD-Induced Hepatic Steatosis

To assess the protective effect of POM on MASLD, we established hepatic steatosis in mice by feeding an HFD and then treating it with POM through tail vein injection (Figure 2a). POM-treated mice showed a significantly lower diet-induced body weight gain (Figure 2b). POM also suppressed dyslipidemia, as evidenced by the lower serum TC, TG, and LDL-C levels (Figure 2c). HFD-induced liver injury was alleviated by POM, as indicated by the decreased serum AST and ALT levels (Figure 2d). Consistently, H&E staining results indicated that POM treatment markedly alleviated the irregular hepatocyte arrangement with ballooning (Figure 2e, yellow arrows). Sirius Red is a strong anionic dye that reacts with basic groups present in the collagen molecule though its sulphonic acid groups, resulting in collagen being dyed red. Sirius Red staining results indicated that POM treatment improved HFD induced liver fibrosis (Figure 2e, red arrows).

Accumulation of intracellular lipids in the liver parenchyma is a major characteristic of MASLD. Oil Red O staining revealed that POM treatment significantly ameliorated lipid accumulation in the livers of HFD-fed mice (Figure 2e). The hepatic TG content in HFD-fed mice was higher than that in mice fed a normal diet, and POM significantly reduced TG levels in the liver (Figure 2f). Similarly, POM treatment significantly decreased liver and serum FFA concentrations (Figure 2g). Hepatocytes are the primary liver cell type and are critical major cells associated with palmitic acid-and oleic acid (PA/OA)-induced lipotoxicity. In vitro, we induced hepatocyte lipid accumulation by treatment with PA/OA and found that adding POM to the medium significantly reduced cellular lipid deposits at concentrations that were not toxic (Supplemental Figure S3a and b).

POM Treatment Upregulates Metabolism Pathways and AMPK Signaling in HFD-Fed Mice

To investigate the potential mechanism of POM in MASLD, we analyzed the liver transcriptomes from normal chow diet-treated, HFD-treated, and HFD+POM-co-treated mice using RNA–seq. Heat map analysis identified 147 genes with >2-fold downregulation and 100 genes with >2-fold upregulation of expression in HFD+POM-cotreated mice compared to HFD-treated mice (Figure 3a). KEGG pathway analysis revealed that metabolic pathways and the AMPK signaling pathway were the main pathways upregulated by POM treatment (Figure 3b). Moreover, lipid and carbohydrate metabolism were strongly affected by POM (Figure 3c).

To confirm the RNA–seq results, we measured the protein and mRNA levels of lipogenic markers in the liver tissue and HepG2 cells. As expected, the expression of fatty acid synthase (FASN), ACC1, and stearoyl-CoA desaturase 1 (SCD1) was markedly reduced by POM treatment in HFD-fed mice (Figure 3d and f). SREBP1c preferentially upregulates transcription of lipid synthesis-related genes in the liver.[32] SREBP1c transcription is triggered by activation of the liver X receptor α (LXRα) activation. During lipogenesis, LXRα regulates various key molecules associated with fatty acid synthesis and hypertriglyceridemia.[33,34] The results showed that protein and mRNA expression levels of SREBP1c and LXRα were strongly downregulated by POM (Figure 3e and f). POM also inhibited the PA/OA-triggered expression of FASN, SCD1, and SREBP1c in HepG2 cells (Supplemental Figure S3c and d). Since LXRα is a nuclear receptor, we analyzed LXRα expression and nuclear translocation in HepG2 cells. PA/OA induced significant upregulation of LXRα expression and nuclear translocation and, as expected, treatment with POM reversed these trends (Supplemental Figure S3e and f). These results suggest that POM improves HFD-induced MASLD partly by inhibiting lipid synthesis.

POM Inhibit Hepatic Lipogenesis by Activating AMPK Signaling

Next, we examined the effects of POM on cholesterol levels and found that POM treatment significantly inhibited HFD-induced liver cholesterol accumulation (Figure 4a). Unlike SREBP1c, SREBP2 preferentially promoted cholesterol synthesis. Mature SREBP2 translocates to the nucleus where it activates the transcription of target genes. One of the target genes of SREBP2 is 3-hydroxy-3-methylglutaryl coenzyme A reductase (HMGCR), which encodes a rate-limiting enzyme for TC biosynthesis.[35] POM inhibited HFD-induced SREBP2 expression and maturation (m-SREBP2) (Figure 4b), and IHC analysis showed that POM significantly inhibited the nuclear translocation of SREBP2 and HMGCR (Figure 4c). AMPK is a critical energy metabolism sensor that regulates hepatic lipid homeostasis by suppressing the synthesis of fatty acids and sterols while stimulating β fatty acid oxidation, which is beneficial for attenuating MASLD progression.[36,37] RNA–seq analysis revealed that the AMPK signaling pathway was the main

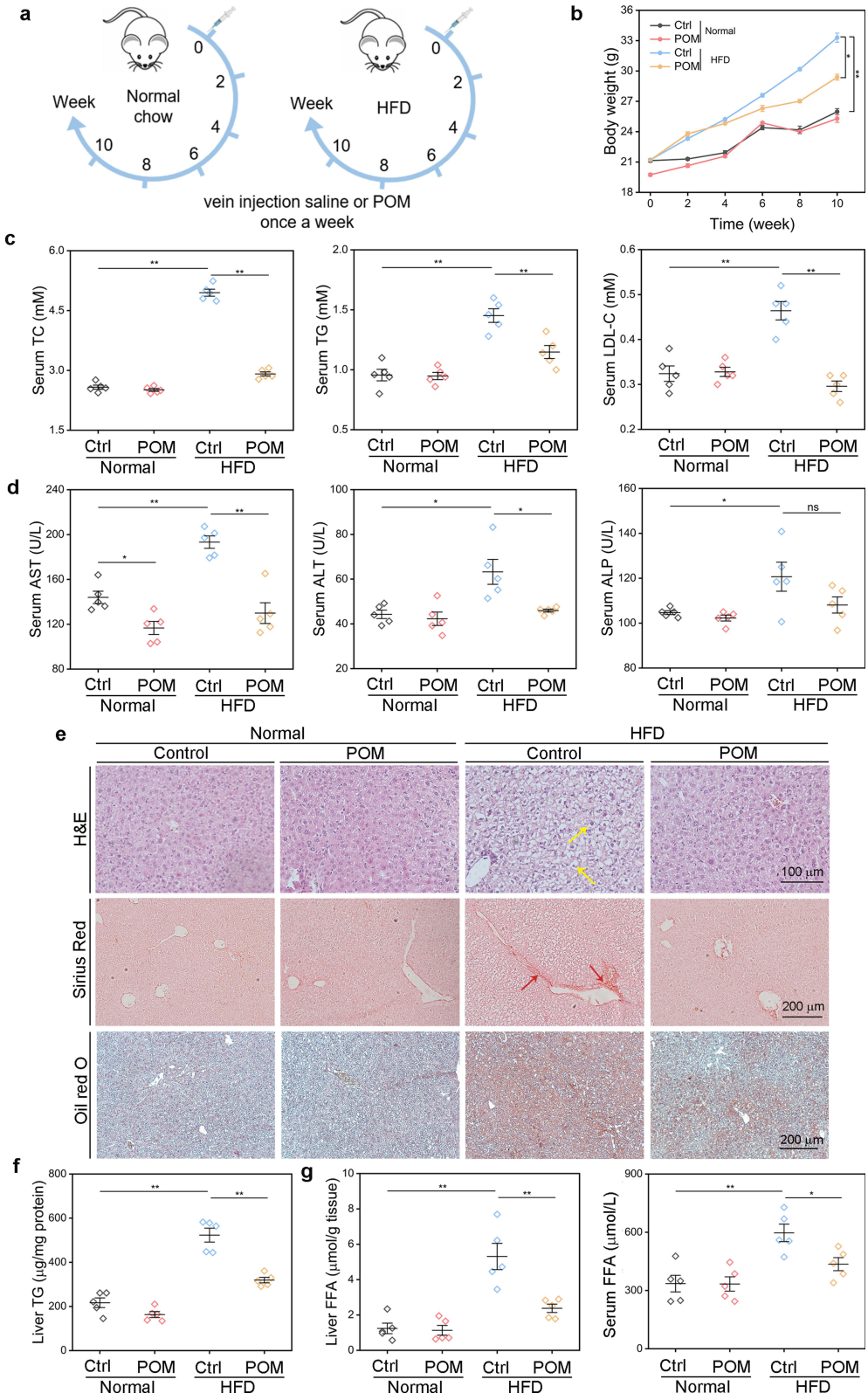

Figure 2 POM attenuate HFD-induced liver injury and lipid accumulation in liver. (**a**) Schematic diagram of experimental design. (**b**) Body weight during treatment with POM. (**c, d**) Serum TC, TG, LDL-C, AST, ALT, and ALP. (**e**) H&E, Sirius Red, and Oil Red O staining of liver sections (yellow arrow: hepatocyte ballooning, red arrow: collagen). (**f**) TG levels in liver samples. (**g**) FFA levels in the liver and serum. *, $P<0.05$; **, $P<0.01$, ns, not significant versus corresponding control ($n = 5$).

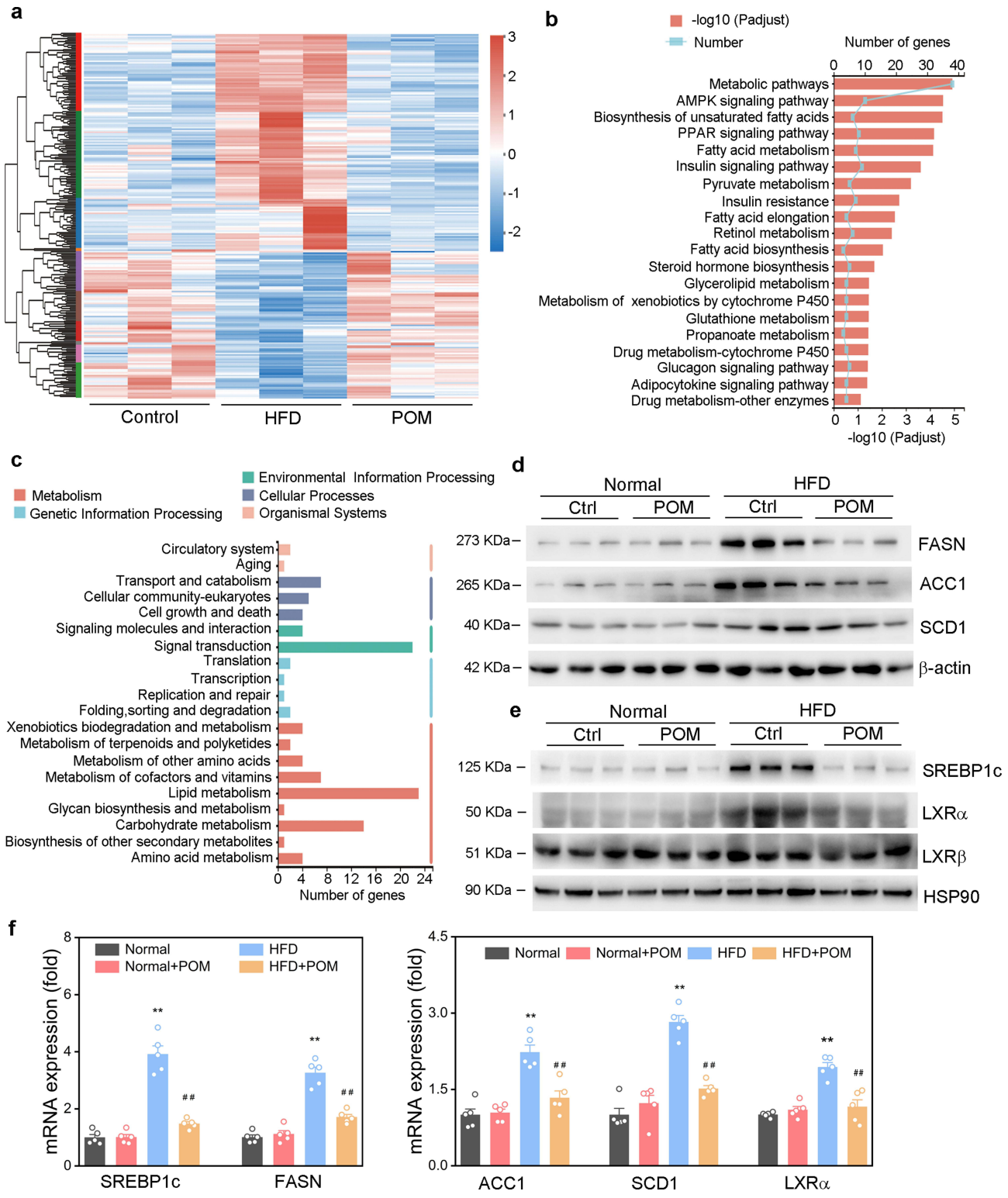

Figure 3 POM inhibit hepatic lipid synthesis-associated protein and gene expression in HFD-administered mice. RNA–seq analysis of HFD-induced liver with or without POM treatment. (**a**) Heat map. (**b**) KEGG enrichment analysis. (**c**) KEGG pathway analysis. (**d, e**) Expression of lipogenesis-related proteins in the liver was assessed by Western blot and (**f**) qRT–PCR. **, $P<0.01$ versus control ($n = 5$). ##, $P<0.01$ versus HFD group ($n = 5$).

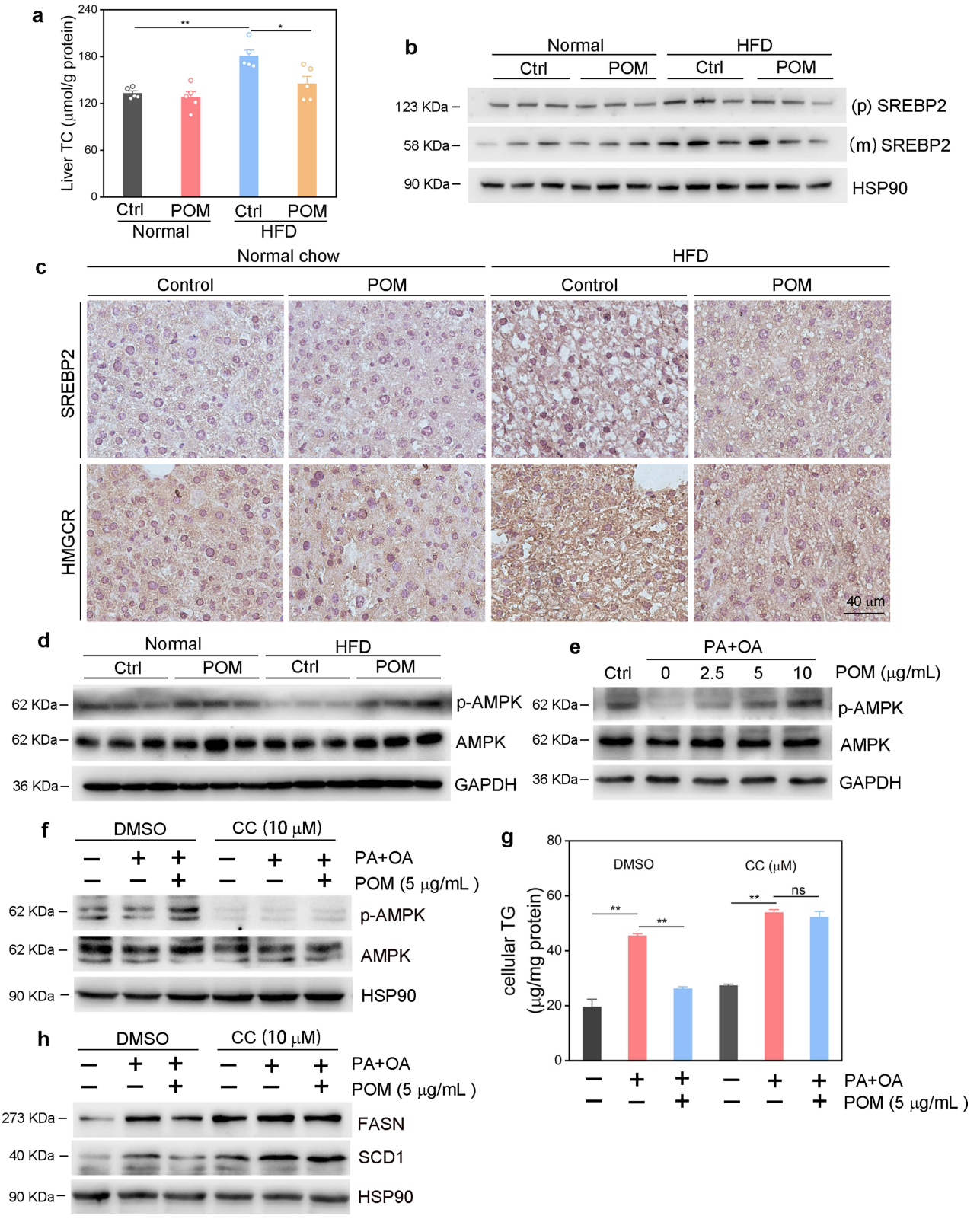

Figure 4 POM inhibit cholesterol synthesis and activate the AMPK signaling pathway. (**a**) TC levels in liver samples. (**b**) Expression of liver precursor (p) or mature (m) SREBP2 was detected by Western blot. (**c**) Expression of liver SREBP2 and HMGCR by IHC. (**d**) Western blot analysis of total or phosphorylated AMPK (p-AMPK) in the liver and (**e**) HepG2 cells with POM treatment with PA/OA stimulation for 24 h. (**f–h**) HepG2 cells were pretreated with the AMPK inhibitor, Compound C (CC), or DMSO for 2 h, and then cells were exposed to PA/OA with or without POM for 24 h. (**f**) Western blot analysis of AMPK signaling. (**g**) TG contents in HepG2 cells. (**h**) Western blot examination of FASN and SCD1. *, $P<0.05$; **, $P<0.01$; ns, not significant versus corresponding control (n = 3–5).

pathway upregulated by POM treatment (Figure 3b). Indeed, we found that POM increased activated AMPK (p-AMPK) in the livers of HFD-fed mice (Figure 4d) and in HepG2 cells induced by PA/OA (Figure 4e).

To determine whether POM reduces lipid accumulation via the AMPK pathway, we used the AMPK inhibitor Compound C to downregulate AMPK activity and then measured the levels of TG and lipid-synthesis-associated gene expression in the presence and absence of POM. Compound C abolished the inhibitory effect of POM on lipid accumulation in HepG2 cells (Figure 4f and g). Notably, the decrease in lipid synthesis-related genes (FASN and SCD1) in hepatocytes mediated by POM was eliminated by Compound C (Figure 4h). Taken together, in vivo and in vitro results indicate that POM inhibited MASLD by activating the AMPK pathway.

POM Ameliorate MCD-Induced Hepatic Steatosis

To determine whether the effects of POM were specific to the HFD model, we evaluated POM treatment in an MASH-like animal model. For more than 40 years, an MCD diet has been used to induce MASLD, which is considered a typical model that develops hepatic histological characteristics of the disease in a short time, including steatosis, inflammation, and fibrosis.[38] To induce liver steatosis and inflammation, we generated MASH-like animals by feeding mice an MCD diet for 4 weeks. Treatment of mice with 50 mg/kg POM by tail vein injection significantly reduced liver injury in MCD-induced mice (Figure 5a), and H&E staining showed that irregular hepatocyte arrangement with inflammation (black arrows) and ballooning degeneration (yellow arrows); were substantially relieved by POM administration. Sirius Red staining showed that MCD-fed mice had more liver fibrosis (collagen fibers are stained red) than mice fed a normal diet. Interestingly, treatment of mice with the MCD diet plus POM attenuated liver fibrosis (Figure 5b), and POM treatment reduced the expression of α-smooth muscle actin (α-SMA) and collagen type I alpha 1 (Col1a1), which are responsible for fibrosis (Figure 5c and d). Our results indicated that POM can prevent or treat MASLD and MASH.

POM Enhance FFA β-Oxidation and Inhibit MCD-Induced Lipotoxicity

MCD impairs fatty acid β-oxidation and very low-density lipoprotein (VLDL) secretion in the liver, thereby driving the progression of liver oxidative stress, inflammatory response, and fibrosis without causing insulin resistance, which is different from HFD-induced MASLD.[39] Oil Red O staining analysis revealed that POM treatment in MCD-induced mice was effective in reducing liver lipid accumulation compared to the MCD diet alone (Figure 6a). As expected, POM-treated mice had significantly decreased liver TG and FFA contents (Figure 6b and c).

To clarify the molecular mechanism by which POM reduces MCD-induced lipid accumulation in the liver, we measured the expression of SIRT1 and its target genes, PPARα, and PGC-1α, which are involved in FFA β-oxidation. Administration of the MCD diet to mice along with POM increased the expression levels of SIRT1, PPARα, and PGC-1α (Figure 6d). To investigate whether POM enhance the activity of PPARα, we measured the mRNA expression levels of CPT-1α and ACOX1, the downstream genes of PPARα. As expected, POM treatment increased the expression levels of CPT-1α and ACOX1 (Figure 6e). The POM treatment results in PA/OA-induced HepG2 cells are consistent with those in vivo (Supplemental Figure S4a–c). These results suggest that POM can partially inhibit MCD-induced lipid accumulation in hepatocytes by promoting fatty acid β-oxidation. Finally, the inflammatory response is one of the mechanisms underlying MCD-induced steatosis, and POM significantly suppressed the inflammatory cytokines induced in the liver and serum by the MCD diet (Figure 6f–h).

POM Increase Antioxidant Levels in Hepatocytes and Reduce Apoptosis

Increased TG levels in the liver can lead to the excessive production of ROS and a decrease in antioxidants, resulting in oxidative stress, which is a critical factor in the induction and promotion of MASH.[40] Hepatic oxidative stress (Figure 7a, red fluorescence) was repressed in MCD-induced POM mice by increasing the expression of antioxidant enzymes, including forkhead box O3a (FoxO3a), superoxide dismutase 1 (SOD1), and SOD2 (Figure 7b and c). Next, we investigated the potential of POM to inhibit lipotoxicity using the TUNEL assay and verified that POM prevented MCD-induced apoptosis in hepatocytes (Figure 7d, red fluorescence). This protective effect of POM was resolved by the inhibition of the Bax/caspase 3 pathway and Bcl-2 (Figure 7e). Our findings indicate that POM can effectively attenuate oxidative stress and inhibit apoptosis induced by an MCD diet.

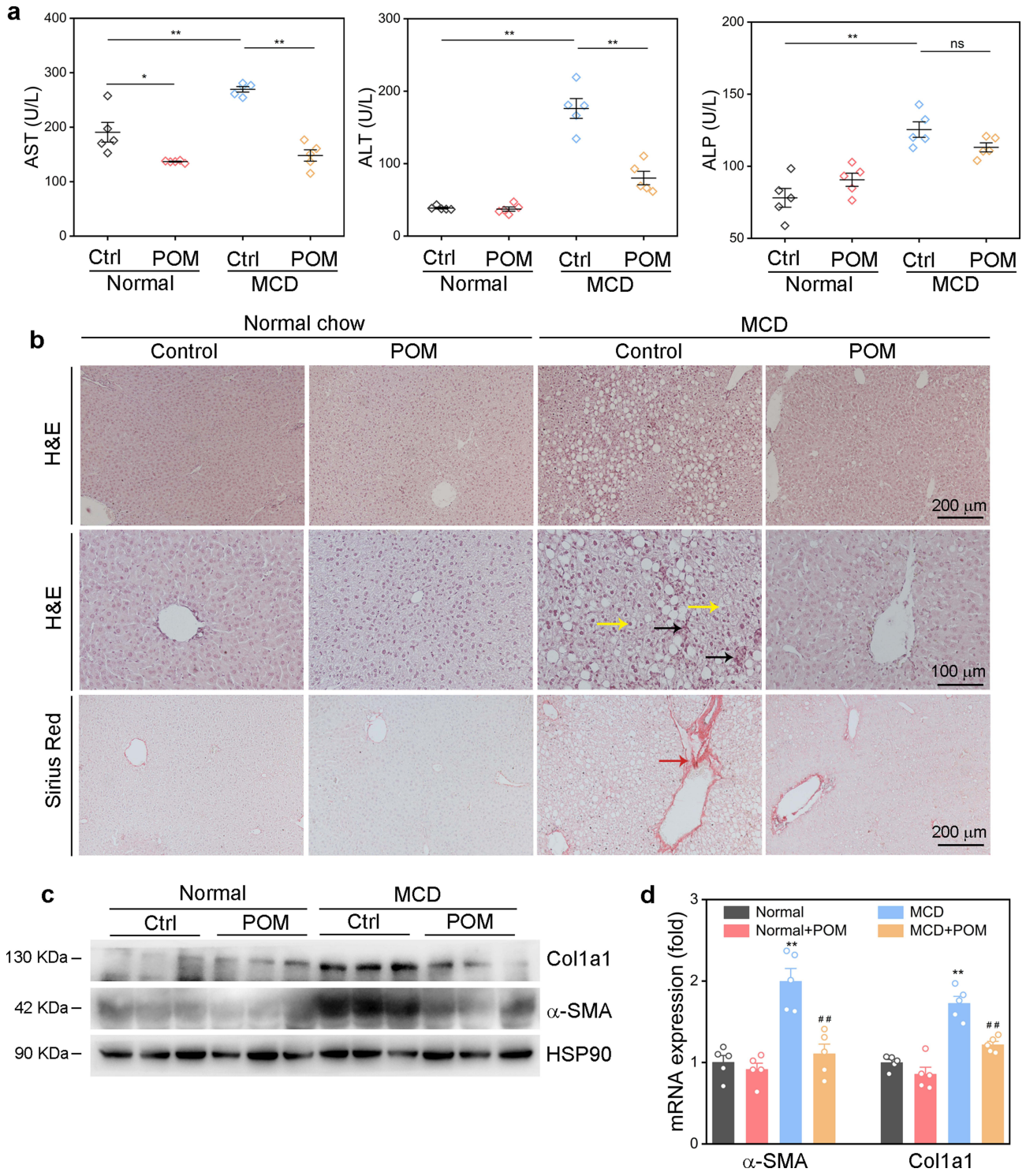

Figure 5 Liver steatosis and injury are lessened by POM in mice administered an MCD diet. (**a**) Serum AST, ALT, and ALP. (**b**) H&E and Sirius Red staining of liver (yellow arrow: hepatocyte ballooning, red arrow: collagen, black arrow: inflammatory cells). (**c**) Levels of α-SMA and Col1a1 assessed by Western blotting. (**d**) mRNA expression of α-SMA and Col1a1 determined using qRT–PCR. *, $P<0.05$; **, $P<0.01$ versus corresponding control ($n = 5$). ##, $P<0.01$ versus MCD group ($n = 5$).

Discussion

With the increasing prevalence of obesity caused by an unhealthy diet, the incidence of MASLD is increasing globally, making it a major global health issue. In some patients with MASLD, simple steatosis can progress to advanced phases with MASH and fibrosis, increasing the risk of cirrhosis and hepatocellular carcinoma risks.[41] However, no effective

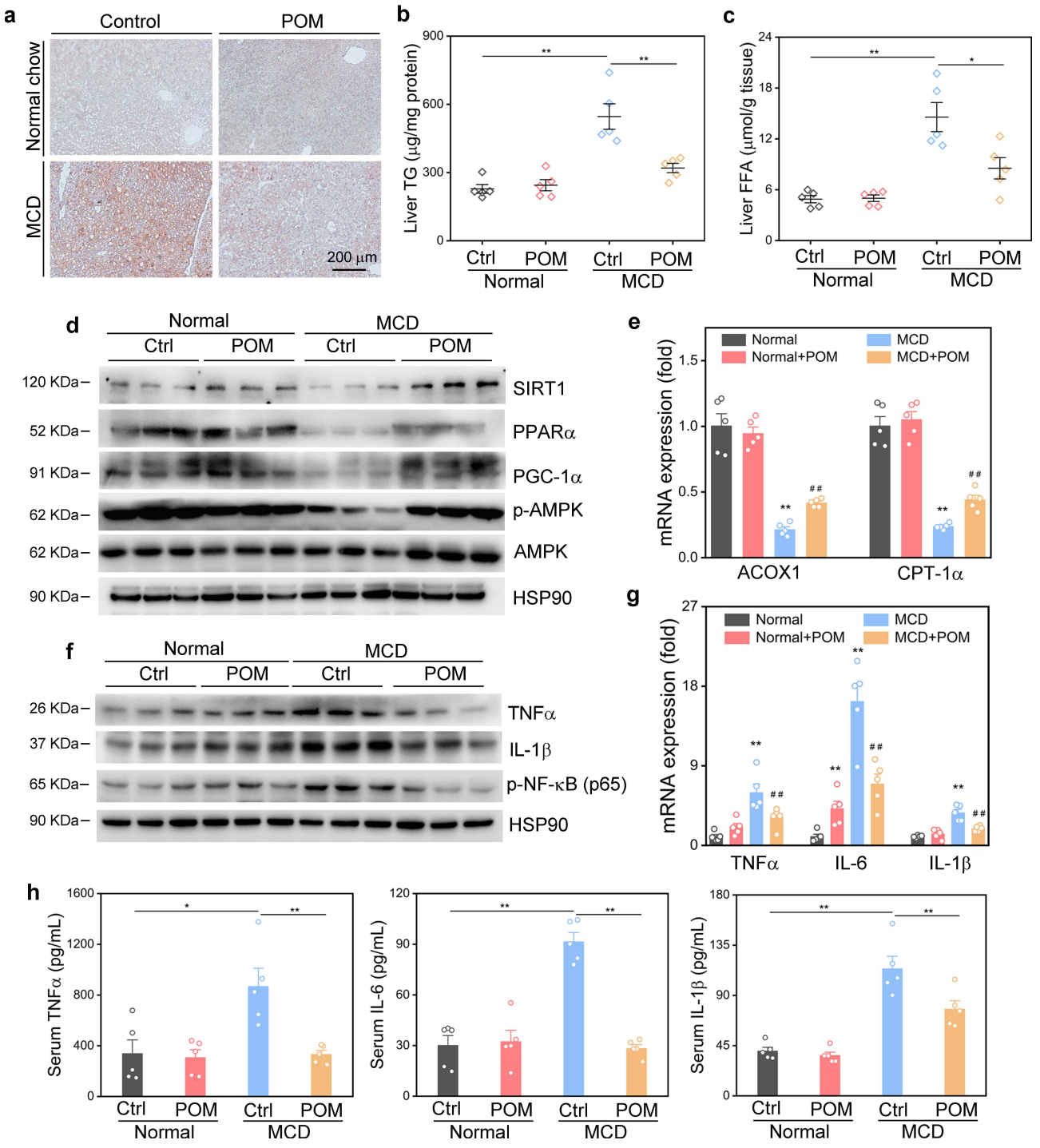

Figure 6 POM inhibit inflammation and promote FFA β-oxidation in MCD-induced mice. (**a**) Staining of liver slices with Oil Red O. (**b**) Liver TG and (**c**) FFA levels. (**d**) Western blot detection of SIRT1, PPARα, PGC-1α, and total or phosphorylated AMPK (p-AMPK) in the liver. (**e**) mRNA expression levels of ACOX1 and CPT-1α determined by qRT–PCR. (**f**) Western blot detection of inflammation-related proteins in the liver. (**g**) qRT–PCR detection of mRNA expression of TNFα, IL-1β, and IL-6. (**h**) ELISA detection of serum TNFα, IL-1β, and IL-6 levels. *, $P<0.05$; **, $P<0.01$; versus corresponding control ($n = 5$). ##, $P<0.01$; versus MCD group ($n = 5$).

treatment is available for MASH prevention or treatment, representing an urgent unmet medical need. In this study, we found that POM can prevent HFD-induced MASLD with simple steatosis as well as MCD-triggered hepatic steatosis, fibrosis, and inflammation in a MASH model. This indicated that POM may be a novel therapeutic approach for MASH.

Lipotoxicity caused by HFD plays a central role in the pathogenesis of MASLD. The liver is the central hub for lipid metabolism, and ameliorating liver lipotoxicity is an effective approach to improve MASLD.[42] Hepatic *de novo*

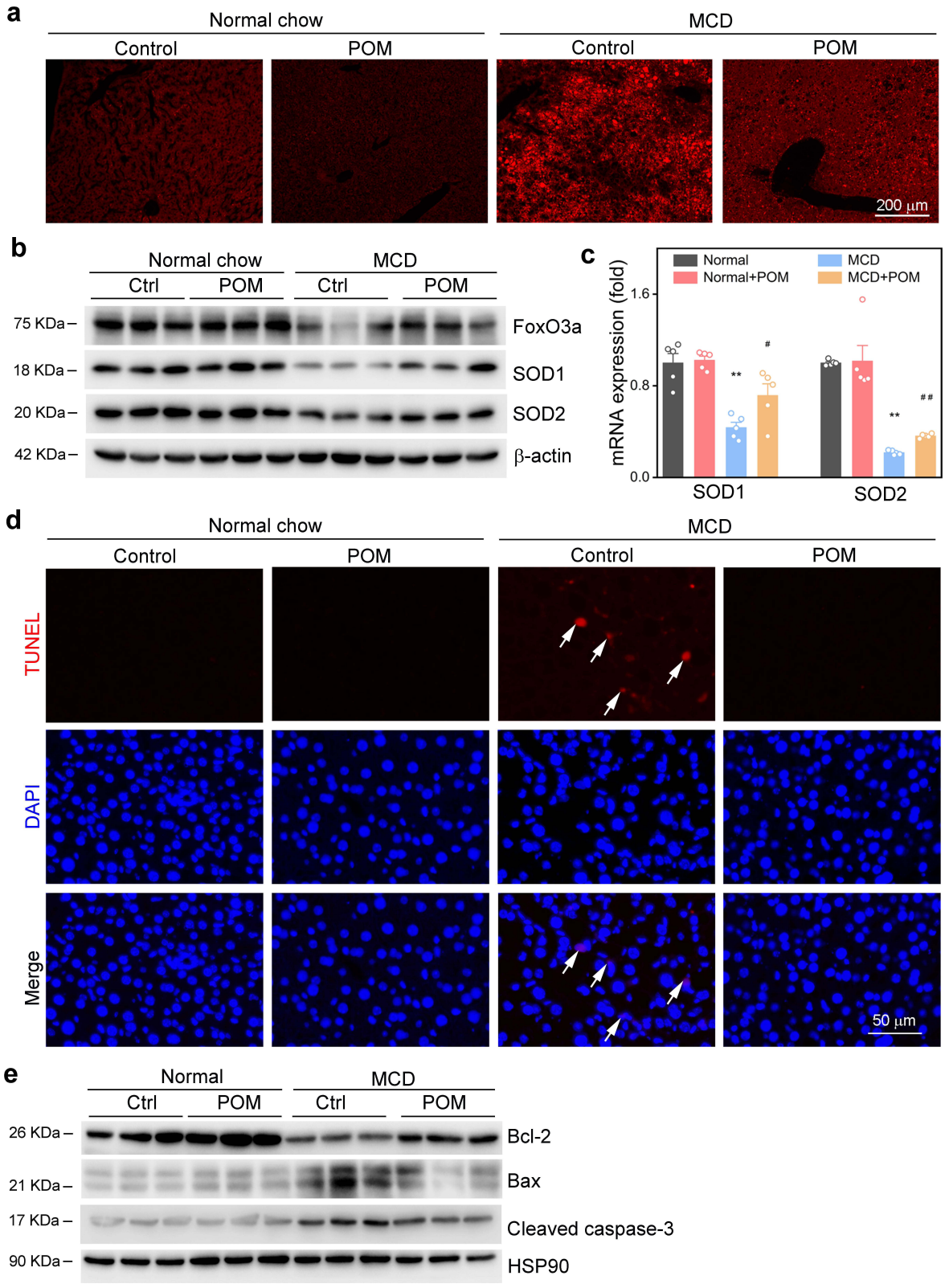

Figure 7 POM attenuate liver oxidative stress and hepatocyte apoptosis in MCD-induced mice. (**a**) ROS levels in the liver assessed via DHE staining. (**b, c**) Western blot or qRT–PCR detection of oxidative stress-related genes in liver. (**d**) TUNEL staining to detect apoptotic cells in liver sections (white arrow: apoptotic cells). (**e**) Western blot detection of apoptosis-related genes in liver. **, $P<0.01$; versus control ($n = 5$). #, $P<0.05$; ##, $P<0.01$; versus MCD group ($n = 5$).

lipogenesis and fatty acid oxidation are important pathways regulating lipid metabolism in the liver. As a transcription factor, SREBP1c is responsible that regulating the expression of FASN, SCD1, and ACC1.[35] Acetyl-CoA is converted to malonyl-CoA by ACC1, and then converted to palmitate by FASN. Finally, palmitate was converted into TG using SCD1.[43] AMPK functions by regulating lipogenesis and lipid oxidation,[44] and, once activated, it can suppress lipogenesis by inhibiting SREBP1c expression as well as its target genes.[45] In this study, we confirmed that the treatment of HFD-triggered mice with POM significantly reduced the accumulation of FFAs, TG, and TC in hepatocytes and reversed the pathological changes associated with MASLD. Mechanistically, POM exerted its therapeutic effects via robust activation of AMPK signaling, which was confirmed by our finding that concurrent treatment with an AMPK inhibitor abolished the molecular and pathological changes in the liver induced by POM.

Hepatic lipid synthesis is related to SREBP2 activity. SREBP2 activates HMGCR expression, a rate-limiting enzyme in cholesterol synthesis, which induces TC biosynthesis in hepatic tissue.[46] Our study showed that the expression of SREBP2 and HMGCR increased in HFD-induced MASLD mice, leading to enhanced liver synthesis of TC, whereas POM supplementation reversed these abnormal trends (Figure 4). AMPK inhibits the nuclear localization of SREBP2, which prevents its transcriptional activator activity of SREBP2; thus, AMPK–SREBP2 signaling is critical for the regulation of cholesterol metabolism.[47] Our findings indicate that the impact of POM on AMPK signaling may restrict hepatic lipid production, thereby protecting the liver from MASLD, thereby protecting the liver from MASLD.

Hepatic β oxidation is a crucial pathway for attenuating the hepatic lipid burden, but a lack of methionine and choline leads to decreased hepatic β oxidation and TG clearance. Fatty acid β oxidation occurs within the mitochondria and is regulated by PPARα and PGC-1α.[48] SIRT1 is only protein identified to be able to deacetylate PGC-1α.[10] SIRT1 is an NAD-dependent deacetylase essential for the pathophysiology of MASLD. Studies have shown that the expression levels of SIRT1, PGC-1α and PPARα in the liver of MASLD mice were downregulated.[16,49–51] Furthermore, the expression of PGC-1α and PPARα target genes was significantly lower in SIRT1 deficient mice.[14] Hepatocyte-specific deletion of SIRT1 leads to failure of PPARα signaling and reduced fatty acid β oxidation.[14] Therefore, in this study, we tested whether SIRT1 was involved in mediating the therapeutic effect of POM on MASLD. Mice fed an MCD diet developed hepatic fat deposition as a result of decreased β oxidation. In our study, treatment of MCD-induced mice with POM significantly reduced the accumulation of FFA and TG in hepatocytes. We also found that MCD impairs hepatic SIRT1, PGC-1α and PPARα expression, while the POM partially restored dysfunctional SIRT1, PPARα, and PGC-1α signaling.

Recent studies have revealed that factors involved in lipid oxidation in the liver are influenced by AMPK.[48] AMPK boosts SIRT1 activity by raising cellular NAD+ levels, leading to the deacetylation and regulation of SIRT1 downstream targets like PGC-1α and the forkhead transcription factors FOXO3a and FOXO1.[13] Although AMPK has been shown to activate PGC-1α through direct phosphorylation,[52] AMPK-induced phosphorylation of PGC-1α is the initiating signal for the subsequent PGC-1α deacetylation that AMPK induces by increasing NAD+ levels within cells.[53] Thus, AMPK activation is a recognized therapeutic target in metabolic disorder-related diseases. However, the potent and ubiquitous functionality of AMPK may lead to undesirable effects. It is worth mentioning that POM specifically activated AMPK in MASLD mice, but not in control animals. Thus, POM might represent a novel approach to modulate AMPK signaling to treat MASLD with an improved therapeutic index compared with other AMPK activators.

In the MCD model, mice first experience hepatic fat accumulation due to impaired mitochondrial β oxidation, followed by an increase in oxidative stress associated with lipid peroxidation, proinflammatory gene expression, and hepatic stellate cells activation.[54,55] Our data showed that POM decreased ROS levels in MCD-induced mice and increased the levels of antioxidants including FoxO3a and SOD. These changes reduced peroxidation-induced apoptosis of hepatocytes to a measurable degree. POM also attenuated the expression of hepatic inflammatory cytokines. Compared with HFD-induced simple steatosis, the MCD diet causes more cell damage and apoptosis.[56] Lipotoxic hepatocellular injury in MCD-fed mice triggers hepatocellular apoptosis, a characteristic marker of steatosis that progresses to steatohepatitis.[57] In this study, we determined that POM protected MCD diet-fed mice against liver injury and hepatocellular apoptosis.

Conclusion

In summary, our study provides convincing evidence of the hepatoprotective effects of POM in MASLD. Our data suggest that the therapeutic effect of POM results mainly from the activation of AMPK signaling, which modulates cellular programs and significantly attenuates hepatic steatosis, the inflammatory response, oxidative stress, and fibrosis. These findings suggest that POM may represent a novel therapeutic approach to intervene early in MASLD and to alleviate the pathological manifestations of MASH. Since POM has not yet advanced to the clinical trial stage, future efforts should focus on precise molecular-level adjustments and investigate the underlying biological mechanisms to enhance their translational application.

Abbreviations

MASLD, metabolic dysfunction-associated steatotic liver disease; POM, polyoxometalates; HFD, high-fat diet; MCD, methionine–choline deficient; MASH, metabolic dysfunction-associated steatohepatitis; PA, palmitic acid; OA, oleic acid; AMPK, AMP-activated protein kinase; SREBP, sterol regulatory element binding protein; SIRT1, Sirtuin 1; TG, triglycerides; ACC1, acetyl-CoA carboxylase 1; PPAR, peroxisome proliferator-activated receptor; PGC-1α, PPARγ coactivator 1α; DHE, dihydroethidium; DMEM, Dulbecco's Modified Eagle's Medium; FBS, fetal bovine serum; GAPDH, glyceraldehyde-3-phosphate dehydrogenase; TC, total cholesterol; LDL-C, low-density lipoprotein cholesterol; AST, aspartate aminotransferase; ALT, alanine aminotransferase; ALP, alkaline phosphatase; FFA, free fatty acid; H&E, hematoxylin and eosin; ROS, reactive oxygen species; KEGG, Kyoto Encyclopedia of Genes and Genomes; IHC, immunohistochemistry; TE, transmission electron microscopy; FT-IR, Fourier-transform infrared spectroscopy; X-ray photoelectron spectroscopy, XPS; FASN, fatty acid synthase SCD1, stearoyl-CoA desaturase 1; LXR, liver X receptor; HMGCR, 3-hydroxy-3-methylglutaryl coenzyme A reductase; CC, Compound C; p-AMPK, phosphorylated AMPK; Col1a1, collagen type I alpha 1; VLDL, very low-density lipoprotein; CPT-1α, carnitine palmitoyl transferase 1α; FoxO3a, forkhead box O3a; SOD, superoxide dismutase; TNFα, tumor necrosis factor α; IL, interleukin.

Acknowledgments

This work was supported by the National Natural Science Foundation of China (U22A20272, 82173807, 82300524, and 52272275), the State Key Laboratory of Functions and Applications of Medicinal Plants, Guizhou Medical University (FAMP202105K) and Innovative Talents Support Program of the Anhui University of Chinese Medicine (2022rczd002).

Disclosure

The authors declare that they have no known competing financial interests or personal relationships that could have influenced the work reported in this study.

References

1. Estes C, Razavi H, Loomba R, et al. Modeling the epidemic of nonalcoholic fatty liver disease demonstrates an exponential increase in burden of disease. *Hepatology*. 2018;67:123–133. doi:10.1002/hep.29466
2. Donnelly KL, Smith CI, Schwarzenberg SJ, et al. Sources of fatty acids stored in liver and secreted via lipoproteins in patients with nonalcoholic fatty liver disease. *J Clin Invest*. 2005;115(5):1343–1351. doi:10.1172/jci23621
3. Adams LA, Angulo P, Lindor KD. Nonalcoholic fatty liver disease. *Cmaj*. 2005;172(7):899–905. doi:10.1503/cmaj.045232
4. Boeckmans J, Natale A, Rombaut M, et al. Anti-NASH drug development hitches a lift on PPAR agonism. *Cells*. 2019;9(1):37. doi:10.3390/cells9010037
5. Reccia I, Kumar J, Akladios C, et al. Non-alcoholic fatty liver disease: a sign of systemic disease. *Metabolism*. 2017;72:94–108. doi:10.1016/j.metabol.2017.04.011
6. Baiceanu A, Mesdom P, Lagouge M, et al. Endoplasmic reticulum proteostasis in hepatic steatosis. *Nat Rev Endocrinol*. 2016;12(12):710–722. doi:10.1038/nrendo.2016.124
7. Cai J, Xu M, Zhang X, et al. Innate immune signaling in nonalcoholic fatty liver disease and cardiovascular diseases. *Annu Rev Pathol*. 2019;14(1):153–184. doi:10.1146/annurev-pathmechdis-012418-013003
8. Castaño D, Larequi E, Belza I, et al. Cardiotrophin-1 eliminates hepatic steatosis in obese mice by mechanisms involving AMPK activation. *J Hepatol*. 2014;60(5):1017–1025. doi:10.1016/j.jhep.2013.12.012
9. Garcia D, Hellberg K, Chaix A, et al. Genetic liver-specific AMPK activation protects against diet-induced obesity and NAFLD. *Cell Rep*. 2019;26(1):192–208.e196. doi:10.1016/j.celrep.2018.12.036

10. Jeninga EH, Schoonjans K, Auwerx J. Reversible acetylation of PGC-1: connecting energy sensors and effectors to guarantee metabolic flexibility. *Oncogene*. 2010;29(33):4617–4624. doi:10.1038/onc.2010.206
11. Hou X, Xu S, Maitland-Toolan KA, et al. SIRT1 regulates hepatocyte lipid metabolism through activating AMP-activated protein kinase. *J Biol Chem*. 2008;283(29):20015–20026. doi:10.1074/jbc.M802187200
12. Li H, Xu M, Lee J, et al. Leucine supplementation increases SIRT1 expression and prevents mitochondrial dysfunction and metabolic disorders in high-fat diet-induced obese mice. *Am J Physiol Endocrinol Metab*. 2012;303(10):E1234–1244. doi:10.1152/ajpendo.00198.2012
13. Cantó C, Gerhart-Hines Z, Feige JN, et al. AMPK regulates energy expenditure by modulating NAD+ metabolism and SIRT1 activity. *Nature*. 2009;458(7241):1056–1060. doi:10.1038/nature07813
14. Purushotham A, Schug TT, Xu Q, et al. Hepatocyte-specific deletion of SIRT1 alters fatty acid metabolism and results in hepatic steatosis and inflammation. *Cell Metab*. 2009;9(4):327–338. doi:10.1016/j.cmet.2009.02.006
15. Vega RB, Huss JM, Kelly DP. The coactivator PGC-1 cooperates with peroxisome proliferator-activated receptor alpha in transcriptional control of nuclear genes encoding mitochondrial fatty acid oxidation enzymes. *Mol Cell Biol*. 2000;20(5):1868–1876. doi:10.1128/mcb.20.5.1868-1876.2000
16. Zhang J, Zhang W, Yang L, et al. Phytochemical gallic acid alleviates nonalcoholic fatty liver disease via AMPK-ACC-PPARa axis through dual regulation of lipid metabolism and mitochondrial function. *Phytomedicine*. 2023;109:154589. doi:10.1016/j.phymed.2022.154589
17. Jin Y, Wang H, Yi K, et al. Applications of nanobiomaterials in the therapy and imaging of acute liver failure. *Nanomicro Lett*. 2020;13:25. doi:10.1007/s40820-020-00550-x
18. Oró D, Yudina T, Fernández-Varo G, et al. Cerium oxide nanoparticles reduce steatosis, portal hypertension and display anti-inflammatory properties in rats with liver fibrosis. *J Hepatol*. 2016;64(3):691–698. doi:10.1016/j.jhep.2015.10.020
19. Cao Y, Xu L, Chen C, et al. Fenofibrate nanoliposome: preparation and its inhibitory effects on nonalcoholic fatty liver disease in mice. *Nanomedicine*. 2016;12(8):2449–2458. doi:10.1016/j.nano.2016.07.002
20. Poilil Surendran S, George Thomas R, Moon MJ, et al. Nanoparticles for the treatment of liver fibrosis. *Int J Nanomed*. 2017;12:6997–7006. doi:10.2147/ijn.S145951
21. Kang JH, Toita R, Murata M. Liver cell-targeted delivery of therapeutic molecules. *Crit Rev Biotechnol*. 2016;36(1):132–143. doi:10.3109/07388551.2014.930017
22. Moosavian SA, Bianconi V, Pirro M, et al. Challenges and pitfalls in the development of liposomal delivery systems for cancer therapy. *Semin Cancer Biol*. 2021;69:337–348. doi:10.1016/j.semcancer.2019.09.025
23. Mukherjee HN. TREATMENT OF CANCER OF THE INTESTINAL TRACT WITH A COMPLEX COMPOUND OF PHOSPHOTUNGSTIC PHOSPHOMOLYBDIC ACIDS AND CAFFEINE. *J Indian Med Assoc*. 1965;44:477–479.
24. Bijelic A, Aureliano M, Rompel A. Polyoxometalates as potential next-generation metallodrugs in the combat against cancer. *Angew Chem Int Ed Engl*. 2019;58(10):2980–2999. doi:10.1002/anie.201803868
25. Ni D, Jiang D, Kutyreff CJ, et al. Molybdenum-based nanoclusters act as antioxidants and ameliorate acute kidney injury in mice. *Nat Commun*. 2018;9(1):5421. doi:10.1038/s41467-018-07890-8
26. Zhou J, Zhao W, Miao Z, et al. Folin-ciocalteu assay inspired polyoxometalate nanoclusters as a renal clearable agent for non-inflammatory photothermal cancer therapy. *ACS Nano*. 2020;14(2):2126–2136. doi:10.1021/acsnano.9b08894
27. Zhao J, Li K, Wan K, et al. Organoplatinum-substituted polyoxometalate inhibits β-amyloid aggregation for alzheimer's therapy. *Angew Chem Int Ed Engl*. 2019;58(50):18032–18039. doi:10.1002/anie.201910521
28. Li S, Qian Q, Ying N, et al. Activation of the AMPK-SIRT1 pathway contributes to protective effects of Salvianolic acid A against lipotoxicity in hepatocytes and NAFLD in mice. *Front Pharmacol*. 2020;11:560905. doi:10.3389/fphar.2020.560905
29. Mei S, Ni HM, Manley S, et al. Differential roles of unsaturated and saturated fatty acids on autophagy and apoptosis in hepatocytes. *J Pharmacol Exp Ther*. 2011;339(2):487–498. doi:10.1124/jpet.111.184341
30. Duan Y, Chen Y, Hu W, et al. Peroxisome Proliferator-activated receptor γ activation by ligands and dephosphorylation induces proprotein convertase subtilisin kexin type 9 and low density lipoprotein receptor expression. *J Biol Chem*. 2012;287(28):23667–23677. doi:10.1074/jbc.M112.350181
31. Yu M, Jiang M, Chen Y, et al. Inhibition of macrophage CD36 expression and cellular oxidized low density lipoprotein (oxLDL) accumulation by tamoxifen: a PEROXISOME PROLIFERATOR-ACTIVATED RECEPTOR (PPAR)γ-DEPENDENT MECHANISM. *J Biol Chem*. 2016;291(33):16977–16989. doi:10.1074/jbc.M116.740092
32. Liang G, Yang J, Horton JD, et al. Diminished hepatic response to fasting/refeeding and liver X receptor agonists in mice with selective deficiency of sterol regulatory element-binding protein-1c. *J Biol Chem*. 2002;277(11):9520–9528. doi:10.1074/jbc.M111421200
33. Laffitte BA, Chao LC, Li J, et al. Activation of liver X receptor improves glucose tolerance through coordinate regulation of glucose metabolism in liver and adipose tissue. *Proc Natl Acad Sci*. 2003;100(9):5419–5424. doi:10.1073/pnas.0830671100
34. Joseph SB, Laffitte BA, Patel PH, et al. Direct and indirect mechanisms for regulation of fatty acid synthase gene expression by liver X receptors. *J Biol Chem*. 2002;277(13):11019–11025. doi:10.1074/jbc.M111041200
35. Horton JD, Goldstein JL, Brown MS. SREBPs: activators of the complete program of cholesterol and fatty acid synthesis in the liver. *J Clin Invest*. 2002;109(9):1125–1131. doi:10.1172/jci15593
36. Herzig S, Shaw RJ. AMPK: guardian of metabolism and mitochondrial homeostasis. *Nat Rev Mol Cell Biol*. 2018;19(2):121–135. doi:10.1038/nrm.2017.95
37. Hardie DG. AMP-activated protein kinase: a master switch in glucose and lipid metabolism. *Rev Endocr Metab Disord*. 2004;5(2):119–125. doi:10.1023/B:REMD.0000021433.63915.bb
38. Weltman MD, Farrell GC, Liddle C. Increased hepatocyte CYP2E1 expression in a rat nutritional model of hepatic steatosis with inflammation. *Gastroenterology*. 1996;111(6):1645–1653. doi:10.1016/s0016-5085(96)70028-8
39. Li H, Toth E, Cherrington NJ. Asking the right questions with animal models: methionine- and choline-deficient model in predicting adverse drug reactions in human NASH. *Toxicol Sci*. 2018;161(1):23–33. doi:10.1093/toxsci/kfx253
40. Mehta K, Van Thiel DH, Shah N, et al. Nonalcoholic fatty liver disease: pathogenesis and the role of antioxidants. *Nutr Rev*. 2002;60(9):289–293. doi:10.1301/002966402320387224
41. Stefan N, Häring HU, Cusi K. Non-alcoholic fatty liver disease: causes, diagnosis, cardiometabolic consequences, and treatment strategies. *Lancet Diabetes Endocrinol*. 2019;7(4):313–324. doi:10.1016/s2213-8587(18)30154-2

42. Li S, Dou X, Ning H, et al. Sirtuin 3 acts as a negative regulator of autophagy dictating hepatocyte susceptibility to lipotoxicity. *Hepatology*. 2017;66(3):936–952. doi:10.1002/hep.29229
43. Ipsen DH, Lykkesfeldt J, Tveden-Nyborg P. Molecular mechanisms of hepatic lipid accumulation in non-alcoholic fatty liver disease. *Cell Mol Life Sci*. 2018;75(18):3313–3327. doi:10.1007/s00018-018-2860-6
44. Minokoshi Y, Kim YB, Peroni OD, et al. Leptin stimulates fatty-acid oxidation by activating AMP-activated protein kinase. *Nature*. 2002;415 (6869):339–343. doi:10.1038/415339a
45. Cantó C, Auwerx J. AMP-activated protein kinase and its downstream transcriptional pathways. *Cell Mol Life Sci*. 2010;67(20):3407–3423. doi:10.1007/s00018-010-0454-z
46. Liu S, Gao Y, Zhang L, et al. Rspo1/Rspo3-LGR4 signaling inhibits hepatic cholesterol synthesis through the AMPKα-SREBP2 pathway. *FASEB j*. 2020;34(11):14946–14959. doi:10.1096/fj.202001234R
47. Wang H, Lin C, Yao J, et al. Deletion of OSBPL2 in auditory cells increases cholesterol biosynthesis and drives reactive oxygen species production by inhibiting AMPK activity. *Cell Death Dis*. 2019;10(9):627. doi:10.1038/s41419-019-1858-9
48. Day EA, Ford RJ, Steinberg GR. AMPK as a therapeutic target for treating metabolic diseases. *Trends Endocrinol Metab*. 2017;28(8):545–560. doi:10.1016/j.tem.2017.05.004
49. Zhai T, Xu W, Liu Y, et al. Honokiol alleviates methionine-choline deficient diet-induced hepatic steatosis and oxidative stress in C57BL/6 mice by regulating CFLAR-JNK pathway. *Oxid Med Cell Longev*. 2020;2020:2313641. doi:10.1155/2020/2313641
50. Zhu S, Guan L, Tan X, et al. Hepatoprotective effect and molecular mechanisms of hengshun aromatic vinegar on non-alcoholic fatty liver disease. *Front Pharmacol*. 2020;11:585582. doi:10.3389/fphar.2020.585582
51. Besse-Patin A, Léveillé M, Oropeza D, et al. Estrogen signals through peroxisome proliferator-activated receptor-γ coactivator 1α to reduce oxidative damage associated with diet-induced fatty liver disease. *Gastroenterology*. 2017;152(1):243–256. doi:10.1053/j.gastro.2016.09.017
52. Jäger S, Handschin C, St-Pierre J, et al. AMP-activated protein kinase (AMPK) action in skeletal muscle via direct phosphorylation of PGC-1alpha. *Proc Natl Acad Sci*. 2007;104(29):12017–12022. doi:10.1073/pnas.0705070104
53. Wenz T. Mitochondria and PGC-1α in aging and age-associated diseases. *J Aging Res*. 2011;2011:810619. doi:10.4061/2011/810619
54. Nomura K, Yamanouchi T. The role of fructose-enriched diets in mechanisms of nonalcoholic fatty liver disease. *J Nutr Biochem*. 2012;23 (3):203–208. doi:10.1016/j.jnutbio.2011.09.006
55. He J, Hu B, Shi X, et al. Activation of the aryl hydrocarbon receptor sensitizes mice to nonalcoholic steatohepatitis by deactivating mitochondrial sirtuin deacetylase Sirt3. *Mol Cell Biol*. 2013;33(10):2047–2055. doi:10.1128/mcb.01658-12
56. Pierce AA, Pickens MK, Siao K, et al. Differential hepatotoxicity of dietary and DNL-derived palmitate in the methionine-choline-deficient model of steatohepatitis. *BMC Gastroenterol*. 2015;15(1):72. doi:10.1186/s12876-015-0298-y
57. Hatting M, Zhao G, Schumacher F, et al. Hepatocyte caspase-8 is an essential modulator of steatohepatitis in rodents. *Hepatology*. 2013;57 (6):2189–2201. doi:10.1002/hep.26271